Aggregation According to Classical Kinetics—From Nucleation to Coarsening

Yossi Farjoun*
Department of Mathematics, Massachusetts Institute of Technology

John C. Neu†
Department of Mathematics, University of California, Berkeley

(Dated: March 4, 2009)

We solve the standard Lifshitz-Slyozov (LS) model with conservation of total particles in the limit of small super-saturation. The new element is an effective initial condition that follows from the initial exhaustion of nucleation as described in a previous paper [1]. The effective initial condition is characterized by a narrow distribution of cluster-sizes, all much larger than critical. In the subsequent solution, one of the LS similarity solutions emerges as the long-time limit, as expected. But our solution tells more. In particular, there is a "growth" era prior to what is usually called "coarsening." During "growth" the clusters (all of nearly the same size much larger than critical) eventually exhaust the super-saturation (the exhaustion of *nucleation* in the previous era results from only a small decrease in super-saturation). This allows the critical size to catch up to the clusters, and the traditional "coarsening" begins: Subcritical clusters dissolve and fuel the growth of the remaining super-critical clusters. Our analysis tracks the evolution of cluster sizes during growth and coarsening by complimentary use of asymptotic and numerical methods. We establish characteristic times and cluster sizes associated with growth and coarsening from physical parameters and the initial super-saturation. The emerging distribution is discontinuous at the largest cluster size, and thus selects the discontinuous LS similarity solution as the long-time limit. There are strong indications that the smooth similarity solution proposed in the original LS paper emerges on a, yet longer, "late-coarsening" time-scale.

PACS numbers: 81.10.-h, 68.43.Jk

Introduction

We analyze the growth of clusters in a monomer bath with conserved total monomer density in the small super-saturation limit. The description of late stage coarsening according to the classic Lifshitz-Slyozov (LS) theory [2] is well known in the literature of aggregation: The number of monomers in the largest clusters increases linearly in time, and the density of clusters shrinks as the smaller clusters dissolve back into monomers. But how does it all begin, starting from pure monomer at "time zero"? In a previous paper [1] the authors predict the cluster size distribution that emerges from the nucleation process, and its long-term limit. In the current paper, the solution of the LS equations, with that long-term limit used as an effective initial condition, is tracked all the way to late stage coarsening. In this way, we obtain a "big picture" of the whole aggregation process, based on classical modeling ideas due to Becker-Döring [3], Zeldovich [4], and Lifshitz-Slyozov [2].

Here is the summary using Fig. (1) as a visual guide. The horizontal axis is the largest cluster size, n_m, the vertical is time t, both with logarithmic scales. This graph of t vs. n_m is based on the quantitative solution of the complete model. The plane is divided into horizontal time-slices, "Creation", "Growth", and "Coarsening." The characteristic time $[t]$ to exhaust nucleation is exponentially large in the initial free energy barrier G_* against nucleation, with $[t] \propto \exp\left(\frac{2}{5}G_*/k_BT\right)$. The timescale $[t]$ is the thickness of the creation time-slice. In this time, the supersaturation undergoes only a small relative decrease and the initial clusters continue rapid growth. For diffusion limited growth in (nearly) constant super-saturation, the number of monomers $n(t)$ in a cluster grows at a rate proportional to cluster radius, so $\dot{n} \propto n^{1/3}$ and it follows that $n(t) \propto t^{3/2}$. In particular, the asymptotic line in the creation time-slice of Fig. 1 has a $2:3$ slope consistent with $n_m^{2/3} \propto \frac{t}{[t]}$. In this way we see that the characteristic size $[n]$ of clusters during the creation era is proportional to $[t]^{3/2} \propto \exp\left(\frac{3}{5}G_*/k_BT\right)$. The width of the cluster size distribution grows more slowly, like $(t/[t])^{1/2}$. Hence, the relative width of the cluster size distribution becomes small during the tail of the creation era, $\frac{t}{[t]} \to \infty$. The actual profile of this narrow distribution is determined from the time history of the nucleation rate per unit volume $j(t)$, derived in [1].

In the next time-slice, labeled "Growth", the nearly homogeneous population of rapidly expanding clusters seriously depletes the super-saturation. This depletion causes their rapid growth to stop when their (common) cluster size reaches $\frac{[n]}{\varepsilon^2}$. Here, ε with $0 < \varepsilon \ll 1$ is the initial super-saturation. In Fig. 1, this arrested growth is represented by the nearly vertical segment. The characteristic time which measures the thickness of the growth time-slice is $\frac{[t]}{\varepsilon^{4/3}}$.

*Electronic address: yfarjoun@math.mit.edu; Corresponding author
†Electronic address: neu@math.berkeley.edu

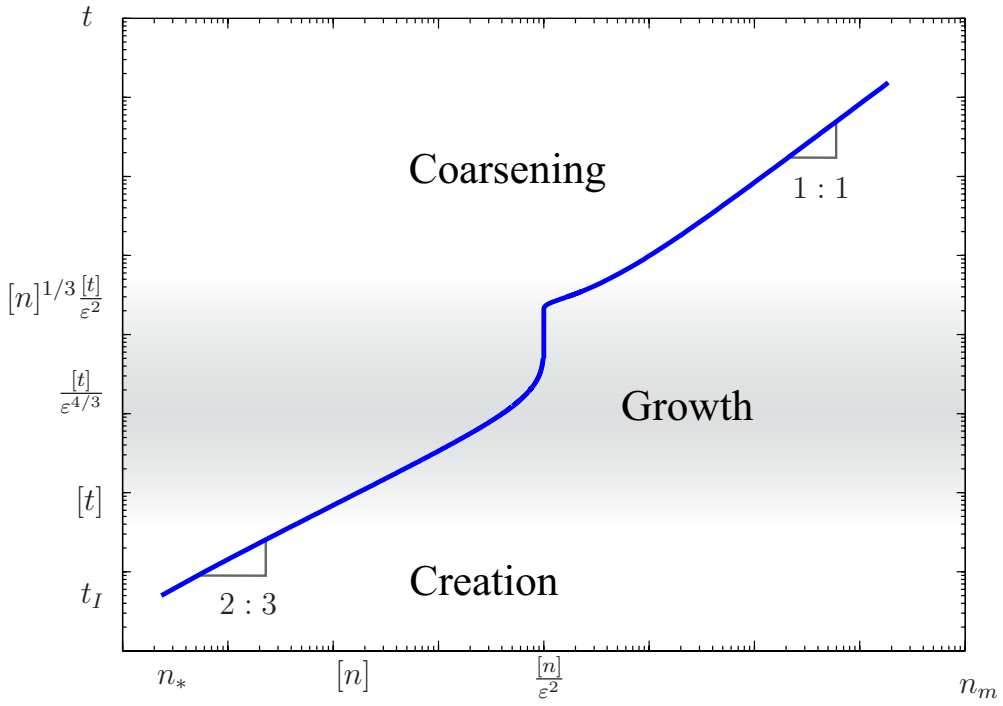

FIG. 1: The graph of time vs. maximal cluster-size in logarithmic scale. The graph shows two obvious regimes (creation and coarsening) separated by a "kink" in the graph (growth and "pre-coarsening") The scales n_*, $[n]$ and $\sigma^3[n]/R\varepsilon^2$ of cluster size are marked in the plot.

The next era, *coarsening*, begins when the critical cluster size, much smaller than the characteristic size during creation and growth, "catches up" with the clusters' size. Clusters smaller than critical shrink, and the monomers they shed are taken up by the larger, growing clusters. Thus, the distribution widens. The characteristic size of the clusters during the coarsening era remains the same as it was during the growth era, but the timescale is much longer: $[n]^{\frac{1}{3}}[t]/\varepsilon^2$.

In *late stage* coarsening, $t \gg [n]^{\frac{1}{3}}[t]/\varepsilon^2$, the cluster size distribution asymptotes to a similarity solution of the LS equations, and we finally reach the stage when n_m is linear in time. Indeed, the asymptotic line in the coarsening time-slice of Fig. 1 has the characteristic $1:1$ slope.

Thus concludes the "brief history" of aggregation according to the classical ideas of BD, Zeldovich, and LS. We highlight some collateral results. First regarding time and size scales: By introducing a physical initial condition that represents the initial nucleation process, we ultimately determine the characteristic time to reach coarsening and the characteristic cluster size, as functions of the physical parameters and initial supersaturation. In particular the time to reach coarsening, $[t]_{\rm c} = [n]^{\frac{1}{3}}[t]/\varepsilon^2$, is exponentially large in the initial free energy barrier G_*, even relative to the time $[t]$ of the creation era. An actual physical time-scale *cannot* result from the LS theory alone. Indeed, the famous similarity solutions result precisely from scale invariance.

This brings us to a peculiar detail: The late-stage coarsening similarity solution that is selected by our solution of the LS equations is discontinuous at the largest cluster size. It is widely believed that the physically correct similarity solution is the smooth, C^∞, one. In the discussion section we propose that during an additional era following coarsening, the distribution evolves further and tends to the smooth C^∞ similarity solution.

The organization of the paper is as follows: In Section I, we review the origins of the cluster size distribution during the tail of the creation era, as set forth in [1]. This, of course, is the effective initial condition for the growth era, treated in Section II. Section III treats the coarsening era and its asymptotic matching with the tail of the growth era. Here there is an additional twist: The coarsening era is evolved numerically, whereas the effective initial condition inherited from the growth era comes from an analytic solution. The switching from analytic to numerical solution is controlled as a function of the numerical resolution, so we have a de-facto "analytic-numerical matching." One corollary of this expanded sense of matching is the analytic determination of a time delay for the onset of coarsening, proportional to $\log\frac{1}{\varepsilon}$.

In Section IV we re-derive the family of similarity so-

lutions using our notation. The discontinuous member of this family is determined and the convergence of the numerical solution to it is verified.

I. THE PHYSICAL MODEL AND EFFECTIVE INITIAL CONDITIONS

In the classic Lifshitz-Slyozov (LS) theory, the number of monomers $n = n(t)$ in a cluster satisfies the ODE of diffusion limited growth:

$$\dot{n} = \mathcal{D}(\eta n^{\frac{1}{3}} - \sigma), \quad \mathcal{D} = \left(3(4\pi)^2\right)^{\frac{1}{3}} D v^{\frac{1}{3}} f_s. \tag{1.1}$$

Here, η is the chemical potential of monomers in the bath (in units of $k_B T$) relative to monomers in the bulk of clusters. When the monomer density f_1 approaches the *saturation density* f_s, for which the monomer bath would be in equilibrium with an "infinite" cluster, we have the asymptotically linear relation

$$\eta = \tfrac{f_1 - f_s}{f_s}. \tag{1.2}$$

In (1.1), σ is the dimensionless surface tension constant so that the interfacial free energy of a cluster with n monomers is $\frac{3}{2} n^{\frac{2}{3}} \sigma k_B T$. In the definition of the rate constant $\mathcal{D}$, D denotes the diffusivity of monomers in the bath and v is the monomer volume inside clusters.

The state variable of the LS equations is the cluster-size distribution $r(n,\, t)$, so that the density of clusters with size n between n_1 and n_2 is $\int_{n_1}^{n_2} r(n,\, t)\, dn$. There are two basic equations: First, the convection PDE

$$\partial_t r + \partial_n \left\{ \mathcal{D}\left(\eta n^{\frac{1}{3}} - \sigma\right) r \right\} = 0, \text{ for } n > 0, \tag{1.3}$$

represents transport of clusters in the space of their size n by the diffusion limited growth "velocity" in (1.1). Second, the conservation of monomers couples the value of the super-saturation, η and the solution. The conservation of monomer is expressed approximately by

$$f = (1+\eta) f_s + \int_0^\infty n\, r(n,\, t)\, dn. \tag{1.4}$$

Here, the total monomer density f, a constant in time, is the sum of monomer density $f_1 = (1+\eta) f_s$ (from (1.2)) in the bath, and the the density of monomers in clusters is approximated by the integral.

In the convection PDE (1.3), σ is positive, so characteristics in the (n,t) plane are *absorbed* by the $n-$axis. Hence, the $n-$axis is a "sink", representing the complete dissolution of subcritical clusters. This is consistent with the assumption that creation of new clusters by fluctuation over the critical size is negligible during the "growth" and "coarsening" eras. In a previous paper [1] we derive scaling units $[t]$, $[r]$, $[n]$ of time t, cluster size n and cluster size density r that characterize the creation era. It is convenient to express the characteristic scales of the growth and coarsening eras as multiples of these creation era scales. Hence, we carry out a preliminary non-dimensionalization of (1.3, 1.4) based on $[t]$, $[r]$, and $[n]$. The unit of chemical potential η is $[\eta] = \varepsilon$, the initial value of chemical potential in the pure monomer bath, before nucleation. The dimensionless equations are

$$\partial_t r + \partial_n \left\{ n^{\frac{1}{3}} r - s \right\} = 0, \quad \text{in } n > 0, \tag{1.5}$$

$$\eta = 1 - \frac{\varepsilon^2}{\sigma^3} \int_0^\infty n\, r\, dn. \tag{1.6}$$

In (1.5), s is the scaled surface tension, exponentially small as $\varepsilon \to 0$ defined in appendix A in (A.4). Equations (1.5, 1.6) are solved for $r(n,\, t)$ subject to an effective initial condition that arises from asymptotic matching with the creation era. In the previous paper we showed that at a range of time t, after nucleation is exhausted, but before the effects of growth change the super-saturation significantly, $r(n,\, t)$ is asymptotic to a narrow distribution is approximated by

$$r(n,\, t) = \begin{cases} N^{-\frac{1}{3}} j\left(\dfrac{N-n}{N^{1/3}}\right), & 0 < N - n < 5N^{\frac{1}{3}} \\ 0, & \text{otherwise.} \end{cases} \tag{1.7}$$

Here, $n = N(t)$ is the size of the largest cluster, approximated by

$$N(t) \sim \left(\tfrac{2}{3} t\right)^{\frac{3}{2}} (\text{for } t = \emptyset(1)). \tag{1.8}$$

The function $j(t)$ is the dimensionless nucleation rate whose graph is shown in Fig. 2. In our previous paper [1] it is shown that $j(t)$ satisfies the integral equation

$$\log j(t) = -\int_0^t \left(\tfrac{2}{3}(t-\tau)\right)^{\frac{3}{2}} j(\tau)\, d\tau. \tag{1.9}$$

Its solution, $j(t)$, decays to zero faster than exponential as $t \to \infty$. For $t \geq 5$, $j(t)$ is a negligible fraction of its initial value, so we truncate the support of $j(t)$ to $0 < t < 5$ for simplicity of presentation. This explains the upper limit $5N^{\frac{1}{3}}$ in (1.7). The reduction in monomer density due to aggregation during the creation era is denoted R and is calculated from j:

$$R = \int_0^\infty j(\tau)\, d\tau \approx 1.7117. \tag{1.10}$$

The value $R \approx 1.7117$ is, of course, a scaled density. To get a physical density one needs to multiply it by $[n][r]$, with $[n]$ and $[r]$ given by (A.2, A.3).

II. GROWTH ERA

During the growth era, the cluster distribution is still approximated by (1.7), but the growth of the largest cluster-size $N(t)$ slows relative to the $t^{3/2}$ growth law (1.8) due to the depletion of supersaturation. Here is a

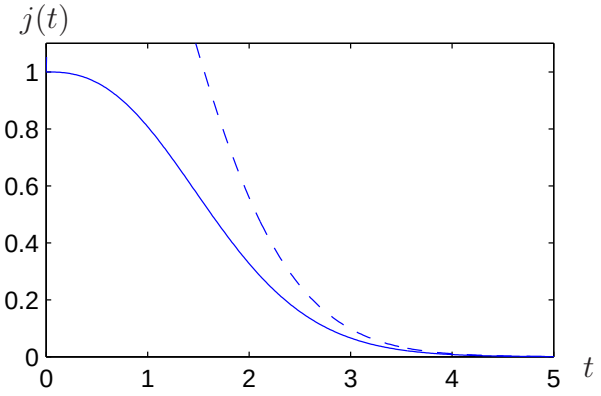

FIG. 2: The solution of Eq. (1.4) is the rate of production of new clusters $j = e^{\delta\eta(t)}$ during the nucleation era. The tail of the flux rate decays super-exponentially in t. The dashed line is the asymptotic result found in [1].

brief summary of the argument. In the convection PDE (1.5), the component $\eta n^{1/3}$ of convection velocity is much greater than one, so the scaled surface tension s is asymptotically negligible. The convection PDE thus reduces asymptotically to

$$\partial_t r + \partial_n \left\{ n^{\frac{1}{3}} r \right\} = 0, \qquad \text{in } n > 0. \tag{2.1}$$

The corresponding *physical* idea is that most of the clusters are much larger than critical. It follows from (2.1) that $n^{1/3}r(n,\, t)$ is constant along characteristics that satisfy

$$\dot{n} = \eta n^{\frac{1}{3}}. \tag{2.2}$$

In (2.2), $\eta = \eta(t)$ decreases from (near) 1 in the beginning of the growth era to (near) 0 at the end in a manner consistent with the conservation identity (1.6). We see that the characteristics determined by (2.2) are *continuations* of the creation era characteristics, carrying the *same* values of $n^{1/3}r$.

This indicates a very simple construction of the asymptotic solution for $r(n,\, t)$ during the growth era. The details are in Appendix B. In summary, $r(n,\, t)$ is concentrated in a narrow front near the largest cluster size N, and there approximation (1.7) applies. What changes is the evolution of $N(t)$, now described by the ODE

$$\dot{N} = N^{\frac{1}{3}} \left(1 - \frac{N}{N_0} \right), \qquad N_0 = \frac{\sigma^3}{\varepsilon^2 R}. \tag{2.3}$$

Here, $1 - \frac{N}{N_0}$ is the value of $\eta(t)$ consistent with the conservation identity (1.6). The solution to ODE (2.3) with $N(0) = 0$ and $N(t) > 0$ for $t > 0$ is given implicitly by

$$\frac{t}{N_0^{\frac{2}{3}}} = \sum_{j=0}^{2} r_j \log \left(1 + r_j \left(\frac{N}{N_0} \right)^{\frac{1}{3}} \right), \tag{2.4}$$

where r_j are the cube roots of -1: $r_0 = e^{i\frac{\pi}{3}}, r_1 = -1, r_2 = e^{-i\frac{\pi}{3}}$. Figure 3 shows this solution as a "world line" in the (n, t) plane (dark line). The shaded area represents the front where $r(n,\, t)$ is concentrated. In the limit $1 \ll t \ll N_0^{2/3}$, (2.4) reduces to $t \sim \frac{3}{2} N^{2/3}$, in agreement with results (1.8) from the creation era.

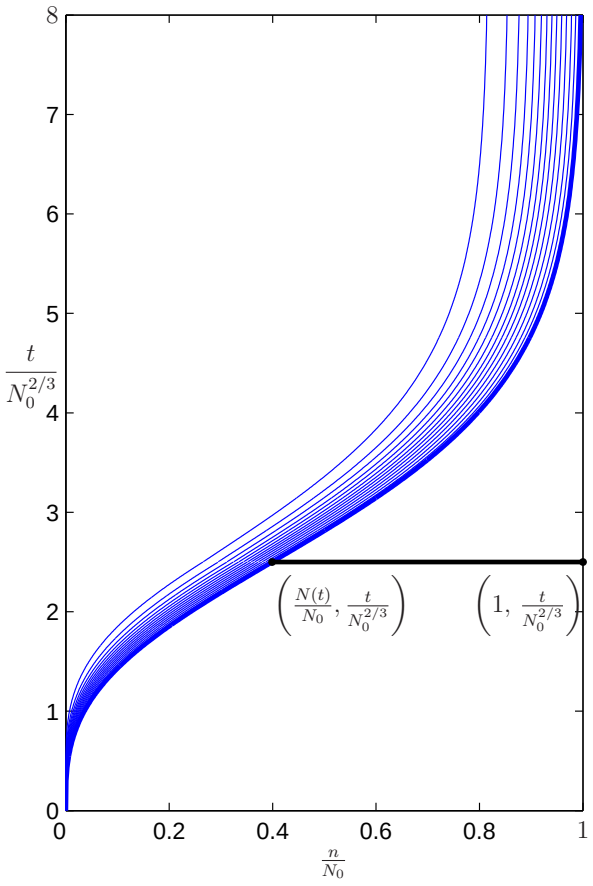

FIG. 3: The "world-lines" of clusters created at the origin. The density of the lines corresponds to the density of clusters at each point. The length of the horizontal line from $(N(t),\, t)$ to $(N_0,\, t)$ (in units of N_0) is the supersaturation η (in units of ε.)

In the opposite limit $t \gg N_0^{2/3}$, which corresponds to the *tail-end* of the growth era, $N(t)$ asymptotes (exponentially) to the constant value $N_0 = \sigma^3/\varepsilon^2 R$. The size distribution asymptotes to

$$r \sim N_0^{-\frac{1}{3}} j \left(\frac{N_0 - n}{N_0^{\frac{1}{3}}} \right), \tag{2.5}$$

independent of time. It is still narrow, with its support is concentrated in an interval of n with $0 < N_0 - n = \emptyset(N_0^{\frac{1}{3}}) \ll N_0$.

Why does the size distribution "stop dead in its tracks"? In Fig. 3, the length of the horizontal line segment from $(N(t)/N_0,\, t)$ to $(1,\, t)$ represents the supersaturation η (in units of ε) at time t. It asymptotes to zero for $t \gg N_0^{2/3}$, and the *truncated* convection velocity $\eta n^{1/3} d$ vanishes with it. The clusters "use up" the

super-saturation that fuels their growth.

In summary, during the growth era, the clusters grow in a relatively narrow distribution until they reach a maximal cluster size $n = N_0$ (in units of $[n]$). The width of the distribution is proportional to $N_0^{1/3}$. The time-scale of the era is $N_0^{2/3}$ (in units of $[t]$), and roughly 10 of these time-units are needed for the narrow, stationary distribution to be established, as seen in Fig. 3. The growth of the clusters is fueled by the supersaturation, which vanishes in an asymptotic sense.

III. COARSENING ERA

The apparent "road-block" to further growth is not the end of the aggregation story. The growth era asymptotics are not uniformly valid as $t/N_0^{2/3} \to \infty$. As η decreases, the exponentially small component s in the full convection velocity $u = \eta n^{\frac{1}{3}} - s$ in (1.3) gains influence until it balances the (now small) $\eta n^{\frac{1}{3}}$. The *critical size* $n_* \equiv (s/\eta)^3$, where $u = 0$, "catches up" with the average cluster size and is now near N_0. Clusters smaller than the critical size n_* shrink, shedding monomers and fueling the continued growth of the clusters larger than n_*. The classic process called *coarsening* has begun. The characteristic time of coarsening, to be determined shortly, is exponentially longer than the characteristic time $[t]\, N_0^{2/3}$ of the growth era. During coarsening, the distribution widens and eventually fills the whole range of cluster sizes from the (growing) maximal size down to zero. The tail of the coarsening era is characterized by convergence to one of the self-similar distributions predicted by Lifshitz and Slyozov.

A. Coarsening era scaling

Relative scaling units[1] of time t and super-saturation η follow from the balance of all three terms in the convection velocity $u = \eta n^{\frac{1}{3}} - s$ in (1.3). The balance between u and s yields N_0/s as the relative unit of time, while balancing $\eta n^{1/3}$ and s gives $s/N_0^{1/3}$ as the relative unit of η. The relative unit R/N_0 of r follows from the balance of the two terms in the RHS of the conservation identity (1.6). The relative and absolute units of n, t, η, and r are summarized in the scaling table:

Variable	n	t	η	r
Relative Unit	$N_0 = \frac{\sigma^3}{\varepsilon^2 R}$	$\frac{N_0}{s}$	$\frac{s}{N_0^{1/3}}$	$\frac{R}{N_0}$
Absolute Unit	$N_0[n]$	$\frac{N_0}{s}[t]$	$\frac{\varepsilon s}{N_0^{1/3}}$	$\frac{R}{N_0}[r]$

The largest cluster size $N(t)$ satisfies ODE (1.1). In the new units this ODE reads

$$\dot{N} = \eta N^{\frac{1}{3}} - 1. \tag{3.1}$$

The scaled PDE (1.3) and conservation identity (1.6) are now

$$\partial_t r + \partial_n \left\{ \left(\eta n^{\frac{1}{3}} - 1 \right) r \right\} = 0, \tag{3.2}$$

in $0 < n < N$, and

$$\frac{s}{N_0^{1/3}} \eta = 1 - \int_0^N n\, r\, dn. \tag{3.3}$$

B. The determination of the supersaturation

In the analysis of the creation and growth eras, the conservation identity explicitly determines η from $r(n,\, t)$. In the coarsening era this straightforward approach fails: By assuming $\varepsilon \ll 1$ we also get $s/N_0^{1/3} \ll 1$, hence the leading order approximation of (3.3) is

$$\int_0^N n\, r\, dn = 1. \tag{3.4}$$

The term containing η disappears. Physically, most of the available monomers are contained in clusters and the super-saturation is vanishingly small. To extract η from $r(n,\, t)$ we differentiate (3.4) with respect to t:

$$\dot{N}\, r(N,t) + \int_0^N n\, \partial_t r\, dn = 0. \tag{3.5}$$

Next, we substitute $\dot{N}$ from (3.1), and $\partial_t r$ from the convection PDE (3.2) into (3.5) and integrate by parts. After some some algebra we find that η can be expressed as

$$\eta = \frac{\int_0^N r\, dn}{\int_0^N n^{\frac{1}{3}} r\, dn}. \tag{3.6}$$

In summary, $r(n,\, t)$ in $0 < n < N$ satisfies the integro-differential equation, consisting of the convection PDE (3.2) with η as in (3.6) and N as in (3.1). An effective initial condition is determined by asymptotic matching with the tail of the growth era. At $n = 0$ the convection velocity is negative, so a boundary condition there is not required.

[1] Since the convection PDE (1.3) and conservation identity (1.6) are non-dimensionalized using nucleation era units $[t]$, $[n]$ from (A.1, A.2) for t and n, and ε is the unit for η, dominant balances in these equations provide scaling units *relative* to those of the nucleation era. For instance the characteristic cluster size relative to $[n]$ is N_0 in (2.3), and the actual unit of n is $N_0[n]$.

C. Changing variables

The growth of the largest cluster size $N(t)$ with time implies that PDE (3.2) has to be solved on a growing interval of n. We simplify the numerical solution by using the following change of variables first:

$$x \equiv \frac{n}{N}, \qquad q(x,\,t) \equiv N r(Nx,t). \tag{3.7}$$

The idea should be clear; The normalized cluster size x ranges in the *fixed* interval $(0,1)$ and q is the distribution of cluster sizes in $x-$space. We multiply r by N so that $q\,dx = r\,dn$. The convection PDE (3.2) for $r(n,\,t)$ transforms into an convection PDE for $q(x,\,t)$,

$$\partial_t q + \partial_x \{w\,q\} = 0, \tag{3.8}$$

in $0 < x < 1$. Here, w is the convection velocity in x space,

$$w = \frac{1}{N}\left(\eta N^{\frac{1}{3}}(x^{\frac{1}{3}} - x) + (x-1)\right). \tag{3.9}$$

Boundary conditions are not required, since w vanishes at $x = 1$ and is negative at $x = 0$. Equation (3.6) translates into a functional dependence of η upon N and moments of q,

$$N^{\frac{1}{3}}\eta = \frac{\int_0^1 q\,dx}{\int_0^1 x^{\frac{1}{3}} q\,dx}. \tag{3.10}$$

The largest cluster size N is easily determined from the conservation identity (3.4) written in terms of q and x:

$$\frac{1}{N} = \int_0^1 x\,q\,dx. \tag{3.11}$$

In summary, both η and N are found explicitly from $q(\cdot,\,t)$ on the interval (0, 1), and this makes (3.8) an explicit integro-differential evolution equation for q. It is convenient to introduce the moments of $q(x,\,t)$ (themselves functions of time):

$$M_0 \equiv \int_0^1 q\,dx, \quad M_{\frac{1}{3}} \equiv \int_0^1 x^{\frac{1}{3}} q\,dx, \quad M_1 \equiv \int_0^1 x\,q\,dx. \tag{3.12}$$

Then (3.10) and (3.11) become

$$N^{\frac{1}{3}}\eta = \frac{M_0}{M_{\frac{1}{3}}}, \quad N = \frac{1}{M_1}, \tag{3.13}$$

and the convection velocity w can be written as

$$w = M_1\left(\frac{M_0}{M_{\frac{1}{3}}}(x^{\frac{1}{3}} - x) + (x-1)\right). \tag{3.14}$$

D. Initial conditions and early widening

The $t \to 0$ limit of the coarsening solution for $r(n,\,t)$ should match distribution (2.5), which characterizes the tail of the growth era. Hence, we have the effective initial condition

$$q(x,\,0) = N_0^{\frac{2}{3}} j\left(N_0^{\frac{2}{3}}(1-x)\right). \tag{3.15}$$

The RHS in (2.5) is translated into x, q variables. Since $N_0 \gg 1$, this initial distribution is a tall spike of height $N_0^{2/3}$ concentrated in a narrow interval of $x-$values near $x = 1$: $0 \le 1 - x \le \emptyset(N_0^{-2/3})$. The initial condition for the largest cluster size N (in coarsening units) is $N(0) = 1$.

To our knowledge, the integro-differential evolution equation for $q(x,\,t)$ does not admit an analytic solution, so a numerical solution is sought. From a numerical point of view, the tall, narrow initial condition (3.15) is not desirable for two reasons: First, it is narrow, with width proportional to $\varepsilon^{\frac{4}{3}}$, and thus resolving it numerically would be difficult (for $\varepsilon \ll 1$). Second, this initial condition depends on ε via the dependence on N_0, thus for every ε we would need to run the computation again. Some preliminary asymptotics fixes both issues and supplies us with a global solution: As long as the distribution remains a narrow spike near $x = 1$, and thus the three moments—M_0, $M_{\frac{1}{3}}$, and M_1—are all near 1, the convection velocity w in (3.14) can be approximated by

$$w \sim x^{\frac{1}{3}} - 1 = \tfrac{1}{3}(x-1) + \emptyset(x-1)^2, \tag{3.16}$$

near $x = 1$. The convection PDE (3.8) with w replaced by its linearization (3.16) can be solved analytically: The "early" evolution of $q(x,\,t)$ based upon the linearized convection velocity (3.16) is given by the widening distribution:

$$q(x,\,t) = N_0^{\frac{2}{3}} e^{-t/3} j\left(N_0^{\frac{2}{3}} e^{-t/3}(1-x)\right). \tag{3.17}$$

This asymptotic distribution matches the effective initial condition (3.15) for $t = 0$, and remains valid as long as the "$x-$width" remains small, $N_0^{-\frac{2}{3}} e^{t/3} \ll 1$.

E. Time-shift and the numerical solution

The strategy now is as follows: First, we assume that our numerical PDE solver accurately resolves a distribution of width δ with $N_0^{-2/3} \ll \delta \ll 1$. From the $\varepsilon-$dependent initial condition (3.15), we evolve $q(x,\,t)$ according to the asymptotic solution (3.17) until the "$x-$width" $N_0^{-2/3} e^{t/3}$ achieves the value δ. This happens at time

$$t = 2\log N_0 + 3\log\tfrac{1}{\delta}. \tag{3.18}$$

The numerical solver takes over for times greater than t in (3.18). The width δ is chosen so that it is much larger than the numerical discretization of x, so that the solution can be resolved, yet much smaller than 1 so that the analytic solution remains valid.

It is convenient to absorb the $\varepsilon-$dependent component $2\log N_0$ in (3.18) by shifting the origin of time. The shifted time is

$$t' = t - 2\log N_0 \tag{3.19}$$

and the numerical solver is turned on at *shifted* time $t' = 3\log\frac{1}{\delta}$, with the effective initial condition

$$q(x,\, t') = \tfrac{1}{\delta} j\left(\tfrac{1}{\delta}\left(1-x\right)\right), \tag{3.20}$$

in $0 < x < 1$. As desired, the time-shift produces an $\varepsilon-$*independent* initial condition for the numerical solver, and thus an $\varepsilon-$independent numerical solution. For a wide range of δ's in $N_0^{-2/3} \ll \delta \ll 1$, the numerical solution at *fixed* t' should be close to the asymptotic solution. We use this later (see Fig. 5) to convince ourselves of the numerical solver's acceptable performance. The details of the numerical solution are spelled out in the Section V.

After finding $q(x,t')$ numerically, we reconstruct $r(n,\, t)$ using (3.7):

$$r(n,t) = \tfrac{1}{N} q\left(\tfrac{n}{N}, t - 2\log N_0\right). \tag{3.21}$$

For $t < 3\log\delta + 2\log N_0$, we use the asymptotic expression (3.17) for q, and for $t > 3\log\delta + 2\log N_0$, we use the numerical solution. Figure 4 shows the *numerical solution* for the coarsening era at various values of the *shifted* time t'.

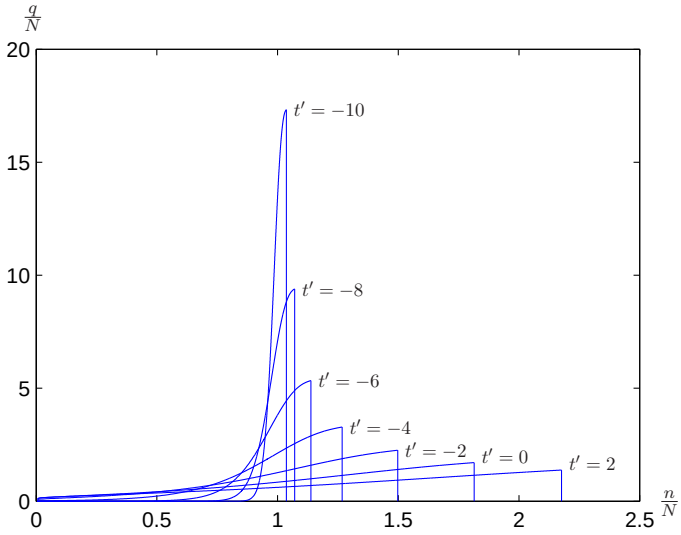

FIG. 4: The numerical solution at various times as found using `clawpack`. Displayed are snapshots from $t' = -10$ to $t' = 2$. The solution continues to evolve after $t' = 2$, as it converges to the similarity solution. Prior to $t' = -10$, the solution is described by the (analytic) asymptotic solution.

The coarsening era solution exhibits three phases: widening, transition, and similarity solution (also called *late stage coarsening*). During the initial widening, the support of the distribution has not yet reached $x = 0$, and the fraction of clusters which have dissolved completely is negligible (See Fig. 6). The widening is accurately described by the asymptotic solution (3.17). During the transition, the support of q reaches down to $x = 0$ and the smaller clusters start dissolving, so the total density of clusters decreases. To resolve this part of the solution the numerical solver is required. The solution is shown in Fig. 4. During the "tail" of coarsening we can observe the convergence of the distribution to a specific similarity solutions of the LS model.

The three phases of the coarsening era can be seen in Fig. 5 which shows the (normalized) distance[2] between the numerical solution and the asymptotic solution (the solid line), and between the numerical solution and the discontinuous similarity solution (the dashed line). Initially, the numerical solution agrees with the asymptotic solution and the normalized distance is negligible. Afterward, in the transition, non-linear effects and the non-zero width of the distribution cause a widening "rift" between the numerical solution and asymptotic one. These non-linear effects also drive the numerical solution towards the similarity solution (which is described in greater detail below), until eventually, the numerical solution is almost indistinguishable from one of the similarity solutions.

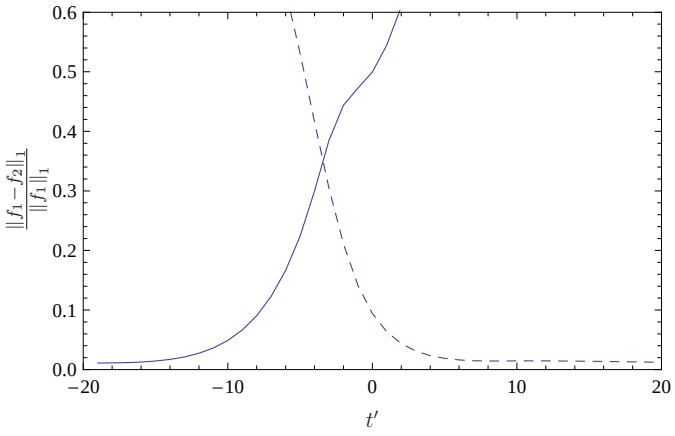

FIG. 5: The normalized distance between the numerical solution and the asymptotic solution given by 3.17 (solid), and the distance between the numerical solution and the discontinuous similarity solution given by (4.14) (dashed).

[2] We use $\frac{\int_0^1 |n(x) - a(x)|\, dx}{\int_0^1 |a(x)|\, dx}$ to measure the distance between a numerical solution $n(x)$ and an asymptotic solution $a(x)$. The normalization is used because the similarity solution decays to 0 as $t \to \infty$ and thus a simple norm might give an impression of convergence when there is none.

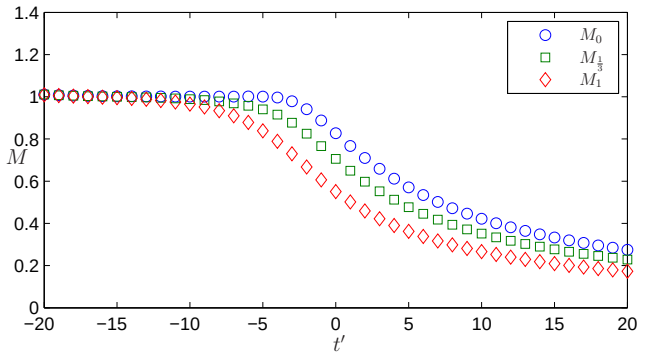

FIG. 6: The three moments M_0, $M_{\frac{1}{3}}$, and M_1 calculated for the numerical solution. Around $t' = -10$, their distance from 1 is noticeable and the asymptotic solution is no longer valid. Around $t' = -5$, M_0 departs from 1 clusters start dissolved at $x = 0$.

IV. SIMILARITY SOLUTIONS

We briefly review the two-parameter family of LS similarity solutions.

The convection PDE (3.8–3.11) admits a separation of variables solution:

$$q(x, t') = c(t')\, P(x). \tag{4.1}$$

We start with the temporal part $c(t')$: In the ODE (3.1) for $N(t)$, substitute $N = 1/M_1$ and $N^{1/3}\eta = M_0/M_{1/3}$ as follows from the two equations in (3.13). We get

$$\dot{M}_1 = M_1^2 \cdot \left(1 - \tfrac{M_0}{M_{\frac{1}{3}}}\right) \tag{4.2}$$

and equations (3.12, 3.13, 4.1, 4.2) imply an ODE for $c(t')$:

$$\dot{c} = -c^2 F \cdot (\mu - 1), \tag{4.3}$$

where F and μ are time independent constants defined by

$$F \equiv \int_0^1 xP\, dx, \quad \mu \equiv \frac{\int_0^1 P\, dx}{\int_0^1 x^{\frac{1}{3}} P\, dx}. \tag{4.4}$$

The solution of ODE (4.3) is

$$c(t') = \frac{1}{F \cdot (\mu - 1)(t' - t_s)}. \tag{4.5}$$

Here, t_s is a time-shift related to the onset of coarsening. It is determined later in the paper using the numerical solution and knowledge of the similarity solution.

Given $c(t')$, we find the spatial part of the similarity solution, $P(x)$. Substituting (4.1) into the convection PDE (3.8), and using ODE (4.3) for c we find an ODE for P:

$$\frac{P_x}{P} = -\frac{\mu\left(2 - \frac{1}{3}x^{-\frac{2}{3}}\right) - 2}{\mu(x^{\frac{1}{3}} - x) + (x - 1)}. \tag{4.6}$$

Figure 7 shows $P(x)$ for different values of μ.

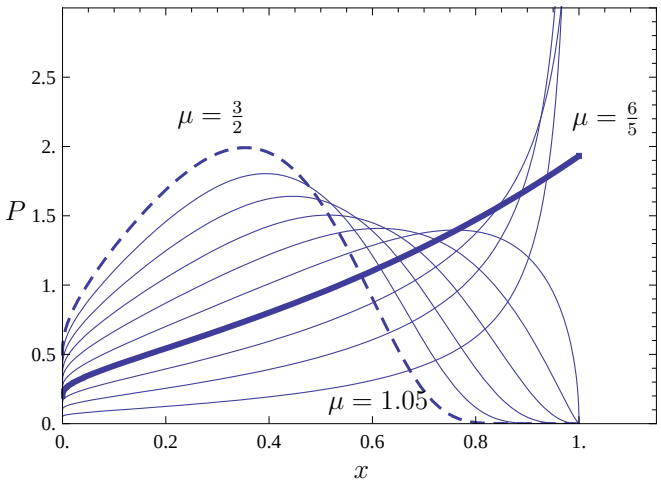

FIG. 7: Profiles $P(x)$ for various values of μ, $1 < \mu \le \frac{3}{2}$. The profiles are normalized so that $\int_0^1 P(x)\, dx = 1$. Specifically, the values of μ in the figure are 1.05 through 1.5 in steps of 0.05. The corresponding orders of contact vary from -0.833 through 0 (bold) and on to ∞ (dashed). A function with order of contact $p \le -1$ is non-integrable, and therefore unphysical.

The parameter μ is related to the order of contact of $P(x)$ (with zero) at $x = 1$. The order of contact is the power p so that

$$P(x) \sim b\,(1 - x)^p \text{ as } x \to 1^-,$$

for some constant $b > 0$. The super-script $(-)$ indicates that the limit is from below. One sees that

$$p = \lim_{x \to 1^-} \tfrac{P_x}{P}(x - 1). \tag{4.7}$$

Substituting (4.6) into (4.7) gives

$$p = \frac{5\mu - 6}{3 - 2\mu}, \quad \text{or equivalently} \quad \mu = \frac{3p + 6}{2p + 5}. \tag{4.8}$$

Since the convection velocity w in (3.14) is regular at $x = 1$, the order of contact of $q(x, t')$ at $x = 1$ is constant, independent of time [5]. The coarsening era solution is discontinuous at $x = 1$, so $p = 0$, and then (4.8) implies $\mu = \frac{6}{5}$. We therefore *expect* the numerical solution to converge to the $\mu = \frac{6}{5}$ similarity solution as $t \to \infty$. This convergence is verified numerically (see Fig. 9.)

For $\mu = \frac{6}{5}$, the similarity solution profile $P(x)$ is:

$$P = \frac{125 \exp\left(-\sqrt{\frac{12}{7}}\left(\coth^{-1}\left(\sqrt{21}\right) - \tanh^{-1}\left(\frac{2x^{1/3}+1}{\sqrt{21}}\right)\right)\right)}{\left(5 - x^{2/3} - x^{1/3}\right)^3}. \tag{4.9}$$

Here, $P(x)$ is normalized so that

$$\int_0^1 P\, dx = 1. \tag{4.10}$$

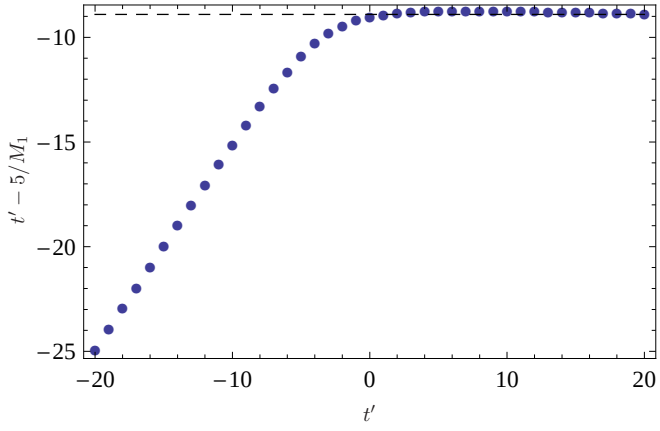

FIG. 8: Finding the time-shift t_s. From around $t' = 0$ and on the value of $t' - \frac{5}{M_1(t')}$ stabilizes on -8.9037.

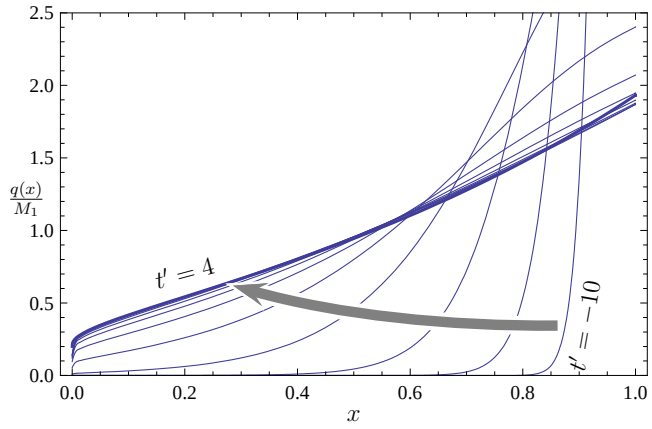

FIG. 9: The numerical solution $q(x, t')$, scaled so that $M_1 = 1$, at different times. Starting on the right at $t' = -10$ in a narrow distribution, and very close to the similarity solution with $\mu = \frac{6}{5}$ (Dark line) at $t' = 4$.

We estimate F in (4.4) for this $P(x)$, numerically. It is

$$F \approx 0.632573 \tag{4.11}$$

The dark line in Fig. 7 shows P with $\mu = \frac{6}{5}$. The dashed line shows the c_∞ solution with $\mu = \frac{3}{2}$. The only parameter that is "matched" to the numerical data is the time-shift, t_s, found via a simple method described next.

A. Asymptotic Matching with Coarsening Era

Finally, we determine the additive time constant t_s in (4.5) by examining the long-time limit of the coarsening era solution. By substituting $q(x, t') = c(t')P(x)$ with $c(t')$ as in (4.5) into (3.12) for M_1, and setting $\mu = \frac{6}{5}$, we find

$$M_1(t') = \frac{5}{(t' - t_s)} \tag{4.12}$$

or equivalently,

$$t_s = t' - \frac{5}{M(t')}. \tag{4.13}$$

In order to estimate t_s, we calculate $M_1(t')$ from the numerical solution and plot the RHS of (4.13) vs. t' in Fig. 8. The horizontal asymptote as $t' \to \infty$ shows that $t_s \approx -8.9037$. In Fig. 5 we see that the numerical solution indeed converges to the similarity solution with $\mu = \frac{6}{5}$ and $t_s = -8.9037$. From $t' = 5$ and on the numerical and similarity solutions are practically indistinguishable. Thus, equations (4.5, 4.9, 4.11) and the value of t_s imply that the coarsening era solution, $q(x, t')$, asymptotes to

$$\frac{625 \exp\left(-2\sqrt{\frac{3}{7}}\left(\coth^{-1}\left(\sqrt{21}\right) - \tanh^{-1}\left(\frac{2x^{1/3}+1}{\sqrt{21}}\right)\right)\right)}{0.632573 \cdot (t' + 8.9037)\left(5 - x^{2/3} - x^{1/3}\right)^3} \tag{4.14}$$

as $t \to \infty$.

V. METHODS

Here we describe the method in which we solved the non-linear convection PDE for the coarsening era. We solve (3.8–3.10) with the initial condition (3.20) using LeVeque's conservation law numerical solver package, `clawpack` [6], using the Riemann problem solver `rp1adecon` (a Riemann solver for conservative convection). Since we expect the solution to start from a narrow and tall distribution near $x = 1$ and widen as t increases, we use a non-uniform grid that becomes more dense towards $x = 1$. Specifically,

$$x_n = \frac{11n}{m + 10n}, \tag{5.1}$$

where $m = 2000$ is the number of grid-cells. Notice that $x_0 = 0$ and $x_m = 1$. This non-uniform grid is chosen so that it has a greater resolution where we expect to find the biggest gradients, i.e. near $x = 1$. The non-uniform grid was implemented using a variable "capacity" in the numerical solver. The capacity of a cell denotes the change in mean value which results from a unit flux into the cell. A non-uniform grid can be implemented on a uniform grid by giving the computational cells that correspond to smaller physical cells a smaller capacity, and the opposite for the larger cells, and adjusting the convection velocity as needed. For more information on implementing non-uniform grid-size in `clawpack` please see [6, Section 6.17].

We start the numerical solution at $t' = -20 = 3 \log \delta$, so $\delta = e^{-20/3} \approx 1.2726 \times 10^{-3}$. The integrals in (3.12) are calculated as Riemann sums[3] By comparing the results

[3] We use Riemann sums and not the trapezoidal rule. In `clawpack`,

to those obtained from a finer mesh and smaller δ, we estimate the relative error to be $\sim 1\%$.

VI. CONCLUSION

The original LS theory with its scale invariance describes late stage self-similar coarsening, but not the actual process of how it arises from the initial condition of pure monomer. In particular, there is no prediction of characteristic cluster size, nor characteristic time that marks the onset of coarsening. This paper, together with its predecessor on the creation era fills this gap in a limited sense: It tells the story of the intermediate processes according to a "classical" aggregation kinetics based on a conservative union of fundamental ideas due to Becker-Döring, Zeldovich, and Lifshitz-Slyozov. As we have seen, there is a succession of three eras, *creation*, *growth*, and *coarsening*, with each consecutive era linked to the previous one by asymptotic matching. In this paper, there is the additional twist of connecting analytic solutions to one universal numerical solution for coarsening.

The characteristic cluster size at the onset of coarsening is

$$[n]_{\rm c} = \frac{\sigma^3}{\varepsilon^2 R}[n], \tag{6.1}$$

where $[n]$ is the characteristic cluster size (A.2) during creation, so the prefactor $\frac{\sigma^3}{\varepsilon^2 R}$ is the relative increase of size between creation and the onset of coarsening. The creation era size $[n]$ itself is dominated by the large exponential $\exp\bigl(\frac{3}{5}G_*/k_BT\bigr)$, so the free energy barrier against nucleation G_* is the most important physical parameter in the determination of the characteristic size of $n_{\rm c}$.

The time to onset of coarsening is a little more subtle than simple scaling alone. From (3.13, 4.12) the largest cluster size (in units of $[n]_{\rm c}$) is

$$N(t') = \tfrac{1}{5}(t' - t_s) \text{ for } t' \gg 1. \tag{6.2}$$

The long time similarity solution in section III can be said to begin around $t' = 0$. This is when the graph of $t' - \frac{5}{M}$ in Fig. 8 becomes constant, as it should for the similarity solution, and when the distance between the numerical solution and the similarity solution is small and shrinking as can be seen in Fig. 5. Recall that t' is the shifted time as in (3.19), so equation (6.2) reproduces the well-known result that the largest clusters size grow linearly with time during late-stage coarsening. The shifted time t' is related to physical time t by translation and scaling, according to

$$t = [t]_{\rm c}\left(t' + 2\log\tfrac{\sigma^3}{\varepsilon^2 R}\right). \tag{6.3}$$

Here, $[t]_{\rm c}$ is the scaling unit of time from the coarsening era,

$$[t]_{\rm c} = \tfrac{N_0}{s}[t] \tag{6.4}$$

or, using s as in (A.4) and $[t]$ as in (A.1),

$$[t]_{\rm c} = \tfrac{\sigma^3}{\varepsilon^2}[n]\left(\frac{1}{Dv^{\frac{1}{3}}f_s}\right). \tag{6.5}$$

The factor $1/Dv^{\frac{1}{3}}f_s$ carries the unit of time. Notice that $[t]_{\rm c}$, like $[n]_{\rm c}$, is proportional to $\exp\bigl(\frac{3}{5}G_*/k_BT\bigr)$. This is exponentially longer than the creation timescale $[t]$ which is proportional to $\exp\bigl(\frac{2}{5}G_*/k_BT\bigr)$. The additive time constant $2\log\frac{\sigma^3}{\varepsilon^2 R}$ in (6.3) comes from (3.19) with $N_0 = \frac{\sigma^3}{\varepsilon^2 R}$. Setting $t' = 0$ in (6.3) we recover the onset of late stage coarsening in physical time,

$$t_{\rm onset} = 2\,[t]_{\rm c}\log\tfrac{\sigma^3}{\varepsilon^2 R}. \tag{6.6}$$

As $\varepsilon \to 0$ the logarithm term is nominally large. But in the "big picture", it is just another prefactor which is overwhelmed by the large exponential $\exp\bigl(\frac{3}{5}G_*/k_BT\bigr)$ in $[t]_{\rm c}$. In summary, the characteristic cluster size and characteristic time associated with the onset of coarsening are both proportional to $\exp\bigl(\frac{3}{5}G_*/k_BT\bigr)$.

VII. DISCUSSION

Although we have described the three eras, as we have set out to do, the aggregation story is not over. According to conventional wisdom, the "correct" similarity solution is the smooth one with $p = \infty$ (and $\mu = \frac{3}{2}$) and not the discontinuous one we found with $p = 0$. In the original LS paper, it is suggested that the (rare) coagulation of large clusters eventually selects the smooth similarity solution. A recent work by Niethammer and Velasquez [7] suggests that screening-induced fluctuations also leads to the selection of the smooth solution.

Even classical kinetics without any additional physics has structure that is not yet fully examined. It can lead to the selection of the smooth solution given sufficiently long time, much longer than $t_{\rm c}$ in (6.4). In particular, the convection PDE boundary value problem for $r(n,t)$ is the lowest order of approximation to a discrete system of ODE's. The next order of approximation introduces an effective diffusion in size space, and this smooths out the discontinuity. Another effect of the discrete kinetics is that the Zeldovich nucleation rate does not abruptly "turn on" at $t = 0$ as we have assumed in our reduced analysis. It has been shown (both analytically [8] and experimentally [9]) that there is a transient during which the nucleation rate *smoothly* increases, with the Zeldovich rate as its long time limit. This is the so-called "ignition transient". Taking this transient into consideration would add a narrow boundary layer to the sharp front, connecting it smoothly to zero. A preliminary analysis shows that a narrow boundary layer about

the cell values represent cell averages, and thus Riemann sum is the correct estimate.

$n = N$ widens on a timescale much longer than $[t]_c$, and the smooth solution results.

In summary, the discontinuous similarity solution is structurally unstable due to a variety of physical and mathematical perturbations. It is now a question of time scales: The mechanism that causes the fastest deviation from the discontinuous solution will determine the timescale of this last era, and will be the main cause for the smoothing of the distribution. This "contest" will be played out in a future paper.

APPENDIX A: COARSENING ERA SCALING

The scales $[t], [r]$, and $[n]$ of time, cluster density and cluster size of the creation era are found (in [1]) to be

$$[t] = (8\pi)^{-\frac{1}{5}} \left\{ \varepsilon^{\frac{3}{5}} \sigma^{-\frac{7}{5}} \right\} e^{\frac{2}{5}\frac{G_*}{k_B T}} \left(D^3 v f_s^3 \omega^2 \right)^{-\frac{1}{5}}, \quad \text{(A.1)}$$

$$[n] = (\pi^{\frac{7}{10}} 2^{\frac{11}{10}} \sqrt{3}) \left\{ \frac{D\varepsilon^4 f_s v^{\frac{1}{3}}}{\sigma^{\frac{7}{2}} \omega} \right\}^{\frac{3}{5}} e^{\frac{3}{5}\frac{G_*}{k_B T}}, \quad \text{(A.2)}$$

$$[r] = (3 \cdot 2^{11} \pi^7)^{-1/5} \left\{ \frac{\sigma^2 \omega^2}{\varepsilon^3 D^2 f_s^2 v^{\frac{2}{3}}} \right\}^{\frac{3}{5}} e^{-\frac{6}{5}\frac{G_*}{k_B T}} (f_s). \quad \text{(A.3)}$$

Here, ε denotes the initial (small) value of the supersaturation $\eta(0)$. In the exponents, the fraction $\frac{\sigma^3}{2\eta^2}$ approximates the initial free energy barrier against nucleation in units of $k_B T$. In the prefactors, ω is the evaporation rate so that $\omega n^{\frac{2}{3}}$ is the rate at which monomers at the surface of an $n-$cluster leave it. The dominant balances leading to these scaling units are based physically upon the Zeldovich rate of nucleation, diffusion limited growth of created clusters, and conservation of monomers. In particular the exponential largeness of characteristic time and cluster size $[t]$ and $[n]$ in ε arise from the exponential smallness of the Zeldovich nucleation rate (proportional to $\exp -\sigma^3/2\eta^3$). The relation $[n] \propto [t]^{\frac{3}{2}}$ as evident from (A.1, A.2) is a signature of diffusion limited growth (in 3D).

The scaled surface tension s in the scaled version of the LS equation (1.5) is given by

$$s = \left(3(4\pi)^2\right)^{\frac{1}{3}} (D v^{\frac{1}{3}} f_s) \tfrac{[t]}{[n]} \sigma. \quad \text{(A.4)}$$

From (A.1, A.2) we see that $s \propto \exp\left(-\frac{1}{5}\sigma^3/2\varepsilon^2\right)$ is exponentially small for $\varepsilon \ll 1$.

APPENDIX B: GROWTH ERA SOLUTION

Let us, for the moment, take $\eta(t)$ as given. The characteristic curve corresponding to the "first" cluster—the one that nucleated at time $t = 0$—is $n = N(t)$, where $N(t)$ satisfies

$$\dot{N} = \eta N^{\frac{1}{3}}, N(0) = 0, \; N(t) > 0 \text{ for } t > 0. \quad \text{(B.1)}$$

The support of $r(n,\, t)$ lies in $\mathcal{R}$:

$$\mathcal{R} \equiv \{(n,\, t) : 0 < n < N(t),\, t > 0\}. \quad \text{(B.2)}$$

In $\mathcal{R}$ the value of $r(n,t)$ is found from

$$r(n,\, t) = n^{-\frac{1}{3}} g(\tau), \quad \text{(B.3)}$$

where $g(\tau)$ is the constant value of $n^{\frac{1}{3}} r(n,\, t)$ along the characteristic curve that has $n(\tau) = 0$. For any point in $\mathcal{R}$, there is one characteristic curve that passes through it, so τ in (B.3) is a function of n and t. Given $\tau = \tau(n,\, t)$, (B.3) is the growth era solution for $r(n,\, t)$ in $\mathcal{R}$.

The asymptotic determinations of $g(\tau)$ and $\tau(n,\, t)$ are simple. It follows from (2.2, B.1) that

$$\tfrac{3}{2} N(t)^{\frac{2}{3}} = \int_0^t \eta(t')dt', \quad \text{(B.4)}$$

$$\tfrac{3}{2} n^{\frac{2}{3}} = \int_{\tau(n,\,t)}^t \eta(t')dt'. \quad \text{(B.5)}$$

Subtracting these equations gives

$$\tfrac{3}{2}\left(N^{\frac{2}{3}} - n^{\frac{2}{3}}\right) = \int_0^{\tau(n,\,t)} \eta(t')dt'. \quad \text{(B.6)}$$

Characteristics with $\tau = \emptyset(1)$ are launched during the creation era, and for these we have that $g(\tau)$ in (B.3) is in fact $j(\tau)$ from (1.9). During creation, $\eta(t)$ (in units of ε) differs from 1 by $\emptyset(\varepsilon^2)$, so for $\tau = \emptyset(1)$, we replace $\eta(t')$ in (B.6) by 1,

$$\tau = \tfrac{3}{2}\left(N^{\frac{2}{3}} - n^{\frac{2}{3}}\right). \quad \text{(B.7)}$$

In the limit $N \gg 1$, the RHS of (B.7) remains $\emptyset(1)$ for $N - n = \emptyset(N^{\frac{1}{3}})$ and in this case we replace the RHS by its linearization about $n = N$, so

$$\tau \sim \tfrac{N-n}{N^{\frac{1}{3}}}. \quad \text{(B.8)}$$

Once we determine $N = N(t)$, (B.8) gives $\tau(n,\, t)$ and the solution for $r(n,\, t)$ in the "front"

$$0 < N(t) - n = \emptyset\left(N(t)\right)^{\frac{1}{3}}. \quad \text{(B.9)}$$

is given by

$$r(n,\, t) \sim N^{-\frac{1}{3}} j\left(\tfrac{N-n}{N^{\frac{1}{3}}}\right). \quad \text{(B.10)}$$

For $N - n \gg N^{\frac{1}{3}}$, $\tau \gg 1$ and $j(\tau)$ asymptotes to zero, corresponding to negligible production of new clusters *after* the creation era.

We complete the story of the growth era by an asymptotic determination of $N(t)$. Since the support of $r(n,\, t)$ is effectively the narrow front (B.9), the conservation identity (1.6) reduces asymptotically to

$$\eta(t) \sim 1 - \tfrac{\varepsilon^2 R}{\sigma^3} N. \quad \text{(B.11)}$$

Here, R is the (scaled) total number of clusters produced during nucleation, given by (1.10). Combining (B.1, B.11) gives a simple ODE for $N(t)$,

$$\dot{N} \sim \left(1 - \tfrac{N}{N_0}\right) N^{\frac{1}{3}}, \tag{B.12}$$

where

$$N_0 \equiv \tfrac{\sigma^3}{\varepsilon^2 R}. \tag{B.13}$$

The solution with $N(0) = 0$ (and $N > 0$ for $t > 0$) is given implicitly by

$$\frac{t}{N_0^{\frac{2}{3}}} = \sum_{j=0}^{2} r_j \log\left(1 + r_j \left(\tfrac{N}{N_0}\right)^{\frac{1}{3}}\right). \tag{B.14}$$

Here, r_j are the cube roots of -1: $r_0 = e^{i\frac{\pi}{3}}, r_1 = -1, r_2 = e^{-i\frac{\pi}{3}}$.

[1] Y. Farjoun and J. C. Neu, Phys. Rev. E **78** (2008), arXiv:cond-mat/0702372.

[2] I. M. Lifshitz and V. V. Slyozov, J. Phys. Chem. Solids **19**, 35 (1961).

[3] R. Becker and W. Döring, Ann. Phys. **24**, 719 (1935).

[4] J. B. Zeldovich, Acta Physiochim, URSS **18**, 1 (1943).

[5] B. Niethammer and R. L. Pego, Journal of Statistical Physics **95**, 867 (1999).

[6] R. J. LeVeque, *Finite-Volume Methods for Hyperbolic Problems* (Cambride University Press, 2002), http://www.amath.washington.edu/~claw/.

[7] B. Niethammer and J. J. L. Velazquez, Indiana Univ. Math. J. **55**, 761 (2006).

[8] J. C. Neu, L. L. Bonilla, and A. Carpio, Phys. Rev. E **71**, 1 (2005), arxiv:cond-mat/0412165.

[9] K. F. Kelton, A. L. Greer, and C. V. Thompson, J. Chem. Phys. **79**, 6261 (1983).